Atoms, molecules, solids, and surfaces: Applications of the generalized gradient approximation for exchange and correlation

John P. Perdew
Department of Physics and Quantum Theory Group, Tulane University, New Orleans, Louisiana 70118

J. A. Chevary and S. H. Vosko
Department of Physics, University of Toronto, Toronto, Ontario, Canada M5S 1A7

Koblar A. Jackson, Mark R. Pederson, and D. J. Singh
Complex Systems Theory Branch, Naval Research Laboratory, Washington, D.C. 20375-5000

Carlos Fiolhais
Department of Physics, University of Coimbra, 3000 Coimbra, Portugal
(Received 7 August 1991; revised manuscript received 10 December 1991)

Generalized gradient approximations (GGA's) seek to improve upon the accuracy of the local-spin-density (LSD) approximation in electronic-structure calculations. Perdew and Wang have developed a GGA based on real-space cutoff of the spurious long-range components of the second-order gradient expansion for the exchange-correlation hole. We have found that this density functional performs well in numerical tests for a variety of systems: (1) Total energies of 30 atoms are highly accurate. (2) Ionization energies and electron affinities are improved in a statistical sense, although significant interconfigurational and interterm errors remain. (3) Accurate atomization energies are found for seven hydrocarbon molecules, with a rms error per bond of 0.1 eV, compared with 0.7 eV for the LSD approximation and 2.4 eV for the Hartree-Fock approximation. (4) For atoms and molecules, there is a cancellation of error between density functionals for exchange and correlation, which is most striking whenever the Hartree-Fock result is furthest from experiment. (5) The surprising LSD underestimation of the lattice constants of Li and Na by 3–4 % is corrected, and the magnetic ground state of solid Fe is restored. (6) The work function, surface energy (neglecting the long-range contribution), and curvature energy of a metallic surface are all slightly reduced in comparison with LSD. Taking account of the positive long-range contribution, we find surface and curvature energies in good agreement with experimental or exact values. Finally, a way is found to visualize and understand the nonlocality of exchange and correlation, its origins, and its physical effects.

I. INTRODUCTION

The ground-state structure of many-electron systems is conveniently calculated within Kohn-Sham density-functional theory.[1,2] Exact in principle, this self-consistent-field theory is usually implemented within the local-spin-density (LSD) approximation for the exchange-correlation energy

$$E_{\rm xc}^{\rm LSD}[n_\uparrow,n_\downarrow]=\int d^3r\, n\varepsilon_{\rm xc}(r_s,\zeta)\ , \tag{1}$$

where $n(\mathbf{r})=n_\uparrow+n_\downarrow$ and n_σ is the density of electrons with spin σ. Here $r_s=(3/4\pi n)^{1/3}$ is the local Seitz radius, $\zeta=(n_\uparrow-n_\downarrow)/n$ is the local polarization, and $\varepsilon_{\rm xc}(r_s,\zeta)$ is the exchange-correlation energy per particle for a uniform electron gas. The LSD approximation, valid in principle for slowly varying densities, has met with impressive practical success, although it underbinds the core electrons in an atom and overbinds the atoms in a molecule or solid.

Using additional information about the electron gas of slowly varying density, Langreth and other authors[3–10] have developed generalized gradient approximations (GGA's):

$$E_{\rm xc}^{\rm GGA}[n_\uparrow,n_\downarrow]=\int d^3r\, f(n_\uparrow,n_\downarrow,\nabla n_\uparrow,\nabla n_\downarrow)\ . \tag{2}$$

These "semilocal" functionals have demonstrated useful improvements over LSD in applications to atoms,[11–13] molecules,[14–20] and solids.[21–25] An extended GGA bibliography is compiled in Ref. 26.

In the original work of Langreth and co-workers,[3–5] a GGA was constructed via cutoff of the spurious small-wave-vector contribution to the Fourier transform of the second-order density-gradient expansion for the exchange-correlation hole around an electron. Perdew and Wang[6–8] (PW GGA-I) argued that the gradient expansion for the hole in real space is an expansion in R (distance from the electron) as well as ∇. They found a more accurate description of exchange by cutting off the spurious long-range contributions in real space, but they continued to use a wave-vector-space cutoff for correla-

tion. Recently, Perdew and Wang[26,27] (PW GGA-II) have presented a unified real-space-cutoff construction of a GGA for exchange and correlation. The PW GGA-II correlation-energy functional has no semiempirical parameter, unlike the PW GGA-I (Ref. 8) and Langreth-Mehl[4,5] functionals. Although the PW GGA-I exchange-energy functional[7,8] could be carried over unchanged into PW GGA-II, slightly greater accuracy is achieved by using the closely similar exchange functional of Becke,[10] to which the PW GGA-II adds theoretical refinements in the small- and large-gradient limits.

A major purpose of this paper is to test PW GGA-II, in comparison with the LSD approximation and PW GGA-I, for a wide range of physical systems: atoms, molecules, solids, and surfaces. A second purpose is to explore the capabilities and limitations of GGA's, or, more generally, of continuum density-functional approximations, for the exchange energy E_x, the correlation energy E_c, and the sum $E_{xc}=E_x+E_c$. (Continuum density functionals, such as LSD or GGA, are those which do not incorporate the derivative discontinuity[28–30] of the exact $E_{xc}[n_\uparrow,n_\downarrow]$.) A third purpose is to develop a qualitative understanding of nonlocality and its physical effects.

Before presenting the PW GGA-II functionals, we discuss their principles of construction and some of their general features. For a density that varies slowly or moderately over space, the exchange and correlation holes surrounding an electron have first-principles expansions in gradients of the density. These expansions to second order predict holes that are fairly realistic close to the electron, but not far away.[31–33] They can be made more realistic via real-space cutoffs chosen to enforce exact properties respected by the zero-order or LSD terms but violated by the second-order expansions: The exchange hole is never positive, and integrates to -1, while the correlation hole integrates to zero. (The nonpositive character of the exchange hole cannot be enforced by a wave-vector-space cutoff—another advantage of real-space analysis.) Sharp or step-function cutoffs have been used in practice.[7,26,27] Thus, the PW GGA-II exchange and correlation holes have *finite* ranges, which shrink as the density gradient at the position of the electron grows. The resulting functionals take the form of Eq. (2). It is found (Sec. VII) that the nonlocalities (∇n dependencies) of PW GGA-II exchange and correlation tend to oppose one another, nearly canceling at low metallic densities. At higher densities, exchange dominates and its full nonlocality is unveiled.

An instructive analogy, which suggests what might be expected from a GGA, is provided by the noninteracting kinetic-energy functional $T_s[n_\uparrow,n_\downarrow]$. Since the exact kinetic-energy density at a point in space is determined by derivatives of the exchange hole about an electron at that point,[34] the second-order gradient expansion of the exchange hole leads to a second-order gradient expansion of T_s. This may also be regarded as the PW GGA for T_s, since the real-space cutoffs occur well outside the position of the electron. It is known that (1) the second-order gradient expansion for $T_s[n_\uparrow,n_\downarrow]$ typically makes an error of less than 1% when applied to the Hartree-Fock electron density of an atom.[35] (2) Its functional derivative $\delta T_s/\delta n_\sigma(\mathbf{r})$ is much less satisfactory: The electron density which solves the Euler equation fails to display the correct shell structure or the correct asymptotic behavior. This density leads to a less realistic kinetic energy than the Hartree-Fock density does.[36] We expect the GGA for exchange and correlation to behave similarly.

The PW GGA-II exchange energy is[26,27]

$$E_x^{\text{PW GGA-II}}[n_\uparrow,n_\downarrow]=\tfrac{1}{2}E_x^{\text{PW GGA-II}}[2n_\uparrow]+\tfrac{1}{2}E_x^{\text{PW GGA-II}}[2n_\downarrow]\ , \tag{3}$$

where

$$E_x^{\text{PW GGA-II}}[n]=\int d^3r\, n\varepsilon_x(r_s,0)F(s)\ , \tag{4}$$

$$\varepsilon_x(r_s,0)=-3k_F/4\pi\ . \tag{5}$$

We use atomic units ($\hbar=e^2=m=1$; energies in hartrees and distances in bohrs). Here,

$$k_F=(3\pi^2n)^{1/3}=1.919\,16/r_s \tag{6}$$

is the local Fermi wave vector and

$$s=|\nabla n|/2k_Fn \tag{7}$$

is a scaled density gradient. The function $F(s)$ is

$$F(s)=\frac{1+0.196\,45s\sinh^{-1}(7.7956s)+(0.2743-0.1508e^{-100s^2})s^2}{1+0.196\,45s\sinh^{-1}(7.7956s)+0.004s^4}\ . \tag{8}$$

For small s,

$$F=1+0.1234s^2+O(s^4)$$

generates the gradient expansion for the exchange energy with the correct coefficient[37] $10C_x/7$, where C_x is the Sham coefficient. Apart from the Gaussian and s^4 terms in Eq. (8), the PW GGA-II and Becke[10] exchange functionals are identical.

The PW GGA-II correlation energy is[26,27]

$$E_c^{\text{PW GGA-II}}[n_\uparrow,n_\downarrow]=\int d^3r\, n[\varepsilon_c(r_s,\zeta)+H(t,r_s,\zeta)]\ , \tag{9}$$

where

$$t=|\nabla n|/2gk_sn \tag{10}$$

is another scaled density gradient,

$$g=[(1+\zeta)^{2/3}+(1-\zeta)^{2/3}]/2\ , \tag{11}$$

and

$$k_s=(4k_F/\pi)^{1/2} \tag{12}$$

is the local screening wave vector. The function H equals H_0+H_1, where

$$H_0=g^3\frac{\beta^2}{2\alpha}\ln\left[1+\frac{2\alpha}{\beta}\frac{t^2+At^4}{1+At^2+A^2t^4}\right], \tag{13}$$

$\alpha=0.09$, $\beta=\nu C_c(0)$, $\nu=(16/\pi)(3\pi^2)^{1/3}$, $C_c(0)=0.004\,235$, $C_x=-0.001\,667$,

$$A=\frac{2\alpha}{\beta}\frac{1}{e^{-2\alpha\varepsilon_c(r_s,\zeta)/(g^3\beta^2)}-1} \tag{14}$$

$$H_1=\nu[C_c(r_s)-C_c(0)-3C_x/7]g^3t^2 \times\exp[-100g^4(k_s^2/k_F^2)t^2]\,. \tag{15}$$

Accurate analytic representations are available for $\varepsilon_c(r_s,\zeta)$ (Refs. 26, 38, and 39) and $C_c(r_s)$.[40] For small gradients with $\zeta=0$, the PW GGA-II exchange-correlation energy correctly[41] reduces to the gradient expansion of Sham with coefficient C_x plus that of Rasolt and Geldart[40] with coefficient $C_c(r_s)$, i.e.,

$$C_{xc}(r_s)=C_x+C_c(r_s)\,.$$

The analytic forms (8) and (13)–(15) fit the numerical results of the real-space cutoff so well that physical properties would be practically unchanged if calculated directly from the numerically defined functions. The form of Eqs. (13) and (14) was suggested[27] by the simpler high-density limit, which arises from the asymptotic scaling behavior of the local[26] and gradient[4,31] contributions to the hole.

PW GGA-II neglects the small "$\nabla\zeta$" terms[42] in the high-density limit of the spin-density gradient expansion[43] (which we have parametrized to fit Table II of Ref. 42):

$$\Delta E_c[n_\uparrow,n_\downarrow] \approx C_c(0)\int d^3r\, n\left\{\frac{-0.458\zeta\nabla\zeta\cdot\left[\frac{\nabla n}{n}\right]}{[n(1-\zeta^2)]^{1/3}}+\frac{(-0.037+0.10\zeta^2)|\nabla\zeta|^2}{n^{1/3}(1-\zeta^2)}\right\}. \tag{16}$$

We shall also test the PW GGA-IIA approximation, which results when the ungeneralized gradient terms of Eq. (16) are added to the PW GGA-II correlation energy of Eq. (9).

An expression for the functional derivative $\delta E_{xc}/\delta n_\sigma(\mathbf{r})$, which serves as an exchange-correlation potential for electrons of spin σ, is presented in Refs. 26 and 27. Subroutines which evaluate the PW GGA-II energy and one-electron potential are available from the authors via electronic mail.

TABLE I. Magnitude ($-E_x^{HF}$) of the exact exchange energy, and difference $-E_{xc}^{DF}+E_x^{HF}$ between exact exchange energy and various density functionals for the exchange-correlation energy, for neutral atoms. All calculations employ Hartree-Fock densities for the observed ground-state configuration and term. (1 hartree =27.2116 eV.) Experimental values from Ref. 11. For comparison, the *total* energy of Zn is -4.89×10^4 eV.

		$-E_{xc}^{DF}+E_x^{HF}$ (eV)					
Atom	$-E_x^{HF}$	PW GGA-IIX	LSD	PW GGA-I	PW GGA-II	PW GGA-IIA	Expt. ($-E_c$)
H	8.50	−0.15	−0.61	0.04	0.03	0.03[a]	0.00
He	27.91	−0.25	−0.80	1.39	1.00	1.00[a]	1.14
Li	48.47	−0.49	−2.52	1.64	1.08	1.02	1.24
Be	72.57	−0.59	−3.55	2.80	1.97	1.97[a]	2.57
B	101.98	−0.75	−4.93	4.06	2.71	2.67	3.40
C	137.40	−0.77	−6.20	5.30	3.65	3.53	4.26
N	179.52	−0.77	−7.53	6.51	4.66	4.44	5.13
O	222.64	−0.59	−8.07	8.93	6.53	6.43	7.02
F	272.42	−0.22	−8.49	11.36	8.55	8.53	8.76
Ne	329.49	0.18	−9.04	13.63	10.59	10.59[a]	10.61
Na	381.44	−0.29	−11.72	14.09	10.78	10.67	10.82
Mg	435.23	−0.40	−13.48	15.64	11.85	11.85[a]	12.07
Al	491.77	−0.70	−15.67	16.76	12.64	12.57	13.07
Si	551.95	−0.94	−17.79	17.96	13.57	13.44	14.17
P	616.10	−1.26	−20.03	19.04	14.46	14.27	15.06
S	680.46	−1.39	−21.38	21.04	16.10	16.03	17.26
Cl	748.77	−1.47	−22.77	22.96	17.77	17.75	19.44
Ar	821.38	−1.68	−24.43	24.65	19.29	19.29[a]	21.42
Cr	1299.93	1.72	−32.32	36.74	31.10	30.48	
Zn	1895.05	5.14	−36.59	51.61	46.65	46.65[a]	
Kr	2554.9	−1.6	−54.4	52	50.6	50.6[a]	
Xe	4876	−6	−94	74	80	80[a]	

[a]Value identically the same as with PW GGA-II.

II. ATOMS

As a first test of our density functionals, we consider the total and electron-removal energies of atoms. The electron density may be constructed via self-consistent solution of either the Hartree-Fock (HF) or Kohn-Sham equations. The former approach, which we adopt here, has certain advantages: Its one-electron potential has the correct asymptotic ($r \to \infty$) limit[30,39] (so that negative-ion solutions exist), and the exact exchange energy E_x^{HF} is evaluated automatically. For a given continuum density-functional approximation, there is some energy difference between the HF and Kohn-Sham densities. For Zn, this difference is about 1 eV in the total energy and about 0.2 eV in the ionization energy. (Full density-functional self-consistency lowers the energy of the neutral atom more than that of the positive ion; compare Table III of Ref. 13 to our Table II.) From the discussion of Sec. I, we expect that the Hartree-Fock density is more realistic and thus more appropriate for comparison with experiment.

Following the approach of Lagowski and Vosko,[11] we have performed self-consistent spin-restricted Hartree-Fock calculations in the central-field approximation for the atoms with $1 \le Z \le 30$ and their first positive and negative ions. Each atom or ion is assigned its observed ground-state configuration and term.[44,45] The nonspherical density is constructed by occupying nonrelativistic spherical-harmonic orbitals in a Slater determinant with $M_L = L$ and $M_S = S$. The scalar-relativistic correction to the total energy is treated as a first-order perturbation.

Table I shows $-E_x^{\mathrm{HF}}$, the magnitude of the exact or Hartree-Fock exchange energy, as well as the difference $-E_{\mathrm{xc}}^{\mathrm{DF}} + E_x^{\mathrm{HF}}$, whose experimental value[11] is the magnitude of the correlation energy. The first density-functional (DF) considered is PW GGA-IIX, the exchange-energy functional of Eqs. (3)–(8). The PW GGA-IIX column of Table I shows an error relative to HF that is typically only a fraction of 1% of the exact exchange energy, as expected.[7,10] The other density functionals considered are the LSD, PW GGA-I, PW GGA-II, and PW GGA-IIA approximations for the exchange-correlation energy, as defined in Sec. I. All take $\varepsilon_c(r_s,\zeta)$ from Ref. 26, except PW GGA-I which employs Ref. 39. Clearly the large total-energy errors of LSD and HF, which are significantly reduced by PW GGA-I[7,8,11–13] are further reduced by PW GGA-II and PW GGA-IIA. The LSD overestimation of the magnitude of the correla-

TABLE II. First ionization energies (I) of 30 atoms. All calculations employ Hartree-Fock densities for the observed ground-state configuration and term of the neutral atom and positive ion, and include scalar relativity as a perturbation. Experimental values from Ref. 44.

		I (eV)						
Atom	Process	HF	PW GGA-IIX	LSD	PW GGA-I	PW GGA-II	PW GGA-IIA	Expt.
H	*s*	13.61	13.45	13.00	13.65	13.63	13.63[a]	13.61
He	*s*	23.45	23.51	24.27	24.96	24.56	24.56[a]	24.59
Li	*s*	5.34	5.42	5.45	5.63	5.61	5.55	5.39
Be	*s*	8.05	8.17	9.01	9.22	9.04	9.14	9.32
B	*p*	7.93	7.92	8.57	8.69	8.57	8.53	8.30
C	*p*	10.78	10.95	11.67	11.65	11.64	11.56	11.26
N	*p*	13.95	14.20	14.92	14.84	14.91	14.82	14.53
O	*p*	11.88	12.38	13.82	14.12	13.76	13.90	13.62
F	*p*	15.70	16.53	17.94	17.94	17.79	17.87	17.42
Ne	*p*	19.82	20.77	22.10	21.99	21.96	21.99	21.56
Na	*s*	4.96	5.19	5.31	5.45	5.36	5.26	5.14
Mg	*s*	6.62	6.89	7.70	7.89	7.64	7.81	7.65
Al	*p*	5.49	5.38	5.98	6.06	6.01	5.95	5.99
Si	*p*	7.64	7.59	8.21	8.25	8.25	8.19	8.15
P	*p*	10.03	9.88	10.51	10.54	10.56	10.51	10.49
S	*p*	9.01	9.07	10.49	10.50	10.30	10.44	10.36
Cl	*p*	11.78	11.88	13.18	13.14	13.05	13.11	12.97
Ar	*p*	14.75	14.71	15.92	15.89	15.85	15.86	15.76
K	*s*	4.02	4.28	4.48	4.60	4.46	4.36	4.34
Ca	*s*	5.14	5.44	6.20	6.36	6.10	6.26	6.11
Sc	*s*	5.38	5.71	6.56	6.73	6.42	6.66	6.54
Ti	*s*	5.54	5.88	6.79	6.97	6.62	6.91	6.82
V	*sd*	6.06	5.76	6.17	6.60	5.96	6.33	6.74
Cr	*s*	6.00	7.06	7.36	7.45	7.23	7.20	6.77
Mn	*s*	5.94	6.29	7.31	7.50	7.06	7.50	7.43
Fe	*s*	6.34	6.84	7.85	8.04	7.59	7.95	7.87
Co	*sd*	8.21	7.57	7.56	8.01	7.47	7.45	7.86
Ni	*sd*	8.11	7.05	7.12	7.62	7.00	6.99	7.63
Cu	*s*	6.56	7.65	8.16	8.32	8.01	7.86	7.73
Zn	*s*	7.78	8.71	9.64	9.82	9.40	9.61	9.39

[a]Value identically the same as with PW GGA-II.

tion energy (by about a factor of 2) is nicely corrected by PW GGA-II.

Tables II and III show the first ionization energy I (neutral atom $\rightarrow$ positive ion) and electron affinity A (negative ion $\rightarrow$ neutral atom), respectively. Four kinds of processes occur: removal of a valence s, p, or d electron, and the "sd" process in which one valence s electron is removed and a second is transferred to a d orbital. All of the continuum density-functional approximations (LSD, PW GGA-I, PW GGA-II, and PW GGA-IIA) display interconfigurational errors:[2,11,13] the tendency to overbind $2p$ and especially $3d$ electrons, leading to a strong overestimation of d removal energies, and (except for PW GGA-I) a strong underestimation of sd energies. There are also some substantial errors which are not interconfigurational in origin (e.g., for the s-electron ionization energy of Cr). We call these "interterm" errors.

Our results for the ionization energies and electron affinities are summarized by the root-mean-square (rms) errors displayed in Table IV. The rows labeled "E_{xc}^{DF}" show the errors when exchange and correlation are both represented by density functionals, as in Tables I–III. The errors are largest for the Hartree-Fock approximation and decrease systematically as we pass to PW GGA-IIX, LSD, PW GGA-I, PW GGA-II, and PW GGA-IIA.

An alternative approach[11,16,23] is simply to add a density functional for correlation to the Hartree-Fock energy, as in the rows of Table IV labeled "$E_x^{HF}+E_c^{DF}$." Although this approach can yield extremely accurate total energies for neutral atoms,[26] it is not as satisfactory as the "E_{xc}^{DF}" approach for valence-electron properties, as demonstrated by the larger errors it makes for the ionization energy and electron affinity in Table IV. Where the Hartree-Fock approximation is furthest from experiment (e.g., for the electron affinities of N, O, F, Fe, Co, and Ni), the PW GGA-IIX approximation is significantly closer, and the PW GGA-II exchange-correlation approximation can be very accurate indeed. Since there is a significant error cancellation[2] between the density-functional descriptions of exchange and correlation, it is best to treat these two together in the same way. The origin of this error cancellation is probably the fact[26,46] that the exact exchange hole can be significantly more long-ranged than the exact exchange-correlation hole or the LSD and GGA holes. The same fact is responsible for the incorrect dissociation limit of spin-restricted Hartree-Fock binding-energy curves for molecules.

Of greater chemical significance than the ionization energy I and electron affinity A of an atom are its electronegativity $(I+A)/2$ and hardness $(I-A)/2$, i.e., the numerical derivatives $-\partial E/\partial N$ and $\frac{1}{2}\partial^2 E/\partial N^2$, where N is the electron number. The charge transfer between two atoms in a molecule or solid is driven by the difference of their electronegativities and opposed by the sum of their hardnesses.[47] Table IV also shows the rms errors for these quantities.

The rms error of the electronegativity is rather small ($\sim$0.2 eV or less) when exchange and correlation are treated in the LSD and especially the PW GGA-II and

TABLE III. Electron affinities (A) of 21 atoms. All calculations employ Hartree-Fock densities for the observed ground-state configuration and term of the neutral atom and negative ion, and include scalar relativity as a perturbation. Experimental values from Ref. 45.

		A (eV)						
Atom	Process	HF	PW GGA-IIX	LSD	PW GGA-I	PW GGA-II	PW GGA-IIA	Expt.
H	s	−0.33	−0.04	0.91	1.1	0.71	0.71[a]	0.75
Li	s	−0.12	−0.03	0.58	0.68	0.53	0.59	0.62
B	p	−0.27	0.18	0.66	0.71	0.62	0.55	0.28
C	p	0.55	1.10	1.67	1.66	1.63	1.55	1.26
N	p	−2.15	−1.23	−0.01	0.25	−0.13	0.00	−0.07
O	p	−0.54	0.73	1.93	1.97	1.74	1.82	1.46
F	p	1.35	2.82	3.97	3.92	3.79	3.81	3.40
Na	s	−0.10	0.05	0.58	0.70	0.56	0.66	0.55
Al	p	0.04	0.21	0.60	0.67	0.60	0.56	0.44
Si	p	0.95	1.04	1.51	1.56	1.53	1.49	1.38
P	p	−0.55	−0.28	0.91	0.96	0.72	0.85	0.75
S	p	0.90	1.24	2.34	2.34	2.19	2.25	2.08
Cl	p	2.56	2.80	3.85	3.85	3.74	3.76	3.62
K	s	−0.08	0.06	0.53	0.64	0.51	0.61	0.50
Ti	d	−1.06	−0.06	0.56	0.44	0.48	0.40	0.08
V	d	−0.76	0.61	1.21	1.05	1.15	1.04	0.52
Cr	s	−0.54	−0.51	0.21	0.37	0.05	0.38	0.67
Fe	d	−2.35	−0.74	0.40	0.35	0.21	0.27	0.16
Co	d	−2.01	0.11	1.21	1.08	1.01	1.05	0.66
Ni	d	−1.70	0.92	1.95	1.79	1.77	1.79	1.16
Cu	s	0.03	0.56	1.15	1.33	1.01	1.16	1.23

[a]Value identically the same as with PW GGA-II.

TABLE IV. Root-mean-square error with respect to experiment for the ionization energy I of the 30 atoms in Table II; for the electron affinity A, electronegativity $(I+A)/2$, and hardness $(I-A)/2$ of the 21 atoms in Table III; and for the s-process electronegativity of the 9 atoms H, Li, Na, K, V, Cr, Co, Ni, and Cu (Table V). Note that the errors are smaller when exchange and correlation are both represented by density functionals (E_{xc}^{DF}), as in Tables I–III, than when a density-functional correlation correction is applied to Hartree-Fock ($E_x^{HF}+E_c^{DF}$).

		rms error of DF (eV)					
Property	E_{xc}	HF	PW GGA-IIX	LSD	PW GGA-I	PW GGA-II	PW GGA-IIA
I	$E_x^{HF}+E_c^{DF}$	· · ·	· · ·	0.43	0.33	0.42	0.33
	E_{xc}^{DF}	1.04	0.77	0.32	0.31	0.30	0.25
A	$E_x^{HF}+E_c^{DF}$	· · ·	· · ·	0.62	0.74	0.84	0.81
	E_{xc}^{DF}	1.51	0.67	0.38	0.34	0.31	0.28
$(I+A)/2$	$E_x^{HF}+E_c^{DF}$	· · ·	· · ·	0.31	0.39	0.52	0.46
	E_{xc}^{DF}	1.11	0.61	0.22	0.28	0.16	0.17
$(I-A)/2$	$E_x^{HF}+E_c^{DF}$	· · ·	· · ·	0.43	0.41	0.40	0.41
	E_{xc}^{DF}	0.57	0.30	0.28	0.17	0.28	0.22
(s,s) or (d,sd)	$E_x^{HF}+E_c^{DF}$	· · ·	· · ·	0.32	0.39	0.54	0.50
$(I+A)/2$	E_{xc}^{DF}	0.88	0.38	0.12	0.24	0.06	0.06

PW GGA-IIA approximations. We explain this as follows: When one electron is removed from an atom or ion, the term (L,S) must change, and so all ionization energies and electron affinities are subject to interterm error. But the electronegativity is the average energy per electron to remove *two* electrons from the negative ion. In many cases (Table V), this process is term conserving, and the errors of LSD and especially PW GGA-II and PW GGA-IIA are then modest. If we consider only the (s,s) and (d,sd) processes, which result in the removal of two valence s electrons, we also eliminate the interconfigurational error. Then the remaining error (Tables IV and V) is small indeed. We propose these s-process electronegativities as a useful atomic testing ground for continuum density functionals, which we suspect cannot otherwise completely escape from interconfigurational and interterm errors. On this ground, PW GGA-II and PW GGA-IIA achieve a rms error of 0.06 eV.

These s-process electronegativities are in fact dominated by exchange and correlation. For a monovalent metal, the electronegativity of the underlying atom is essentially the same as the work function or electronegativity of the metallic crystal,[48] which arises largely from exchange and correlation. [The other contributions are smaller and tend to cancel one another, as shown by Table III of Ref. 49 or Fig. 4(a) of Ref. 50.]

A real atomic density has a cusp at the nucleus, but PW GGA-II works at least as well for cuspless model densities (Table VI).

III. MOLECULES

Hydrocarbon molecules are good choices for testing density functionals. Abundant experimental data, includ-

TABLE V. Electronegativities for the neutral atoms with $1 \le Z \le 30$ for which the first positive and negative ions have the same term (L,S). These density-functional results are free from the interterm errors that bedevil the ionization energies I and electron affinities A of Tables II and III.

			Term-conserving $(I+A)/2$ (eV)						
Atom	Term	Process	HF	PW GGA-IIX	LSD	PW GGA-I	PW GGA-II	PW GGA-IIA	Expt.
H	^1S	s,s	6.64	6.71	6.96	7.4	7.17	7.17[a]	7.18
Li	^1S	s,s	2.61	2.69	3.02	3.15	3.07	3.07[a]	3.01
N	^3P	p,p	5.90	6.48	7.45	7.54	7.39	7.41	7.23
Na	^1S	s,s	2.43	2.62	2.95	3.07	2.96	2.96[a]	2.84
P	^3P	p,p	4.74	4.80	5.71	5.75	5.64	5.68	5.62
K	^1S	s,s	1.97	2.17	2.51	2.62	2.48	2.48[a]	2.42
Ti	^4F	d,s	2.24	2.91	3.68	3.70	3.55	3.66	3.45
V	^5D	d,sd	2.65	3.19	3.69	3.82	3.55	3.69	3.63
Cr	^6S	s,s	2.73	3.28	3.78	3.91	3.64	3.79	3.72
Co	^3F	d,sd	3.10	3.84	4.38	4.55	4.24	4.25	4.26
Ni	^2D	d,sd	3.20	3.98	4.53	4.70	4.39	4.39	4.40
Cu	^1S	s,s	3.29	4.10	4.66	4.82	4.51	4.51[a]	4.48

[a]Value identically the same as with PW GGA-II.

TABLE VI. Exchange (E_x) and exchange-correlation (E_{xc}) energies for cuspless one-electron densities $n(r)=(\alpha^3/32\pi)(1+\alpha r)e^{-\alpha r}$, $\zeta=1$. Here r_s characterizes the maximum density $n(0)=3/4\pi r_s^3$.

	$-E_x$ (eV)			$-E_{xc}$ (eV)		
r_s (bohrs)	LSD	PW GGA-II	Exact	LSD	PW GGA-II	Exact
1	9.90	11.25	11.60	10.59	11.48	11.60
2	4.95	5.63	5.80	5.46	5.82	5.80
4	2.48	2.81	2.90	2.83	2.97	2.90
6	1.65	1.87	1.93	1.93	2.01	1.93

ing very accurate atomization energies,[16] are available. Pederson, Jackson, and Pickett[51] have studied the set of molecules listed in Table VII using LSD, within the parametrization of Ref. 39. The optimized LSD bond lengths make errors of only 1% or 2%, in comparison with experiment. This level of agreement is typical for structural parameters calculated in LSD.

LSD-calculated atomization energies for the molecules of Table VII are much less satisfactory, however. These are typically 10–15 % greater than experimental values. It is this property that we wish to address with the generalized gradient approximations (GGA's). Previous GGA calculations of atomization energies for molecules[14–20] and solids[21–23] have demonstrated considerable improvement over LSD.

The calculations of Tables VII and VIII were performed using a finite cluster, local Gaussian-orbital procedure.[51,52] The method uses a highly accurate numerical integration scheme[52] to evaluate the total energy and matrix-element integrals. In this scheme, the integration mesh is systematically refined to provide essentially arbitrary accuracy for the various integrals. One advantage of the computational procedure is that it allows the Kohn-Sham potential to be used in the calculation, without further approximation. The numerical accuracy of the calculations is then limited only to basis-set completeness, which, in principle, can be systematically controlled.

Except for C_{60}, we have used very large single Gaussian basis sets, consisting of eighteen *single* s-type Gaussians, nine p-type Gaussians, and four d-type Gaussians on each carbon and hydrogen atom. This amounts to a total of 65 functions per atom. To illustrate convergence of the atomization energies, we discuss calculations performed on CH_4 with this basis as well as two smaller basis sets. The smallest basis set, consisting of seven s-type, four p-type, and two d-type *contracted* Gaussian orbitals, gave an atomization energy of 19.94 eV. A larger set, consisting of ten s-type, four r^2 s-type, eight p-type, and four d-type *single* Gaussians led to an atomization energy of 20.11 eV. Finally, the largest set, described above, gave 20.09 eV. Based on this result and similar results for the other systems discussed below, we believe that the atomization energies reported in Table VII are accurate to at least 0.05 eV/atom. For the C_{60} molecular calculation, we have used the smallest basis set.

To obtain the GGA atomization energies for the molecules in Table VII, optimized geometries should be found from self-consistent GGA calculations. Fan and Ziegler[18] have shown, however, that the GGA atomization energies found in this way are essentially indistinguishable from those obtained from a much simpler procedure in which the GGA total energy is evaluated using the LSD electron density and geometry. Because of its simplicity, we use this non-self-consistent approach here.

Calculated atomization energies are shown in Table VII. The density-functional calculations for the carbon atom were performed for the potential of the spherical atom, for which the $2p_x^{\uparrow}$, $2p_y^{\uparrow}$, and $2p_z^{\uparrow}$ orbitals have equal occupation numbers, $\frac{2}{3}$ of an electron each. The nonspherical atom was then constructed by assigning unit occupation to the $2p_x^{\uparrow}$ and $2p_y^{\uparrow}$ orbitals, and zero occupa-

TABLE VII. Atomization energies of seven hydrocarbon molecules and the root-mean-square error per bond relative to experiment. A single, double, or triple bond is counted as one bond. LSD electron densities and geometries are employed in all calculations except HF (Ref. 16). Since the calculated atomization energies are for static molecules, the zero-point vibrational energy has been removed from the experimental values (Ref. 16). The antiferromagnetic (AF) singlet LSD solution is used to represent C_2. (1 eV = 23.06 kcal/mole.)

		Atomization energy (eV)					
Molecule	Number of bonds	HF	PW GGA-IIX	LSD	PW GGA-I	PW GGA-II	Expt.
H_2	1	3.63	3.67	4.89	4.80	4.55	4.75
C_2 (AF)	1	0.73	5.0	7.51	6.62	6.55	6.36
C_2H_2	3	13.00	14.88	20.02	18.20	18.09	17.69
CH_4	4	14.39	14.82	20.09	19.29	18.33	18.40
C_2H_4	5	18.71	20.23	27.51	26.83	24.92	24.65
C_2H_6	7	24.16	25.04	34.48	31.57	31.24	31.22
C_6H_6	12	45.19	49.49	68.42	61.25	61.34	59.67
rms error/bond		2.40	1.00	0.68	0.23	0.13	

TABLE VIII. Total energy of the molecule C_2 measured from the total energy of the antiferromagnetic (AF) singlet, which we take to represent the experimental ground state. The experimental singlet-triplet splitting is from Ref. 54.

	Energy relative to AF singlet (eV)			
	LSD	PW GGA-I	PW GGA-II	Expt.
Nonmagnetic singlet $^1\Sigma_g^+[(\pi_u^\uparrow)^2(\pi_u^\downarrow)^2]$	0.22	0.34	0.35	
Triplet $^3\Pi_u[(\pi_u^\uparrow)^2\pi_u^\downarrow\sigma_g^\uparrow]$	−0.19	−0.17	−0.21	+0.09

tion to the $2p_z^\uparrow$; its total energy is lower than that of the spherical carbon atom by 0.00 eV in LSD, 0.11 eV in PW GGA-I, and 0.10 eV in PW GGA-II. (With spherical harmonic orbitals [$m_l=-1$ and 0] in place of cubic harmonics, the PW GGA-II energy would be lower than that of the spherical atom by only 0.01 eV.)

For the seven molecules shown in Table VII, the rms error per bond is 2.4 eV for Hartree-Fock, 0.7 eV for LSD, 0.2 eV for PW GGA-I, and only 0.1 eV for PW GGA-II. Because the atomization energies of molecules are nearly additive over bonds, we expect that PW GGA-II energies will achieve this level of accuracy for all hydrocarbons.

The cancellation of error between density-functional approximations for exchange and correlation is evident for molecules, as it was for atoms. Another feature of the atomic results carries over to molecules: When Hartree-Fock is a good zero-order approximation, the exchange-only density functional PW GGA-IIX emulates Hartree-Fock energies, although the PW GGA-IIX results fall somewhat closer to experiment. When Hartree-Fock is a poor zeroth-order approximation (C_2), the PW GGA-IIX results fall *much* closer to experiment.

For C_2H_6 (ethane), the structure in which the hydrogen triads are staggered lies only 0.13 eV below that in which they are eclipsed. This experimental energy difference[53] is correctly predicted by both LSD (Ref. 51) and PW GGA-II.

Six of the seven molecules in Table VII have closed subshells. C_2, however, has several low-lying excited states. The experimental ground state[54] is a spin singlet, but the density-functional approximations that we tested place the triplet state lower in energy (Table VIII). The LSD total energy of the singlet is reduced by a broken-symmetry antiferromagnetic (AF) solution, in which equal but opposite spin moments appear. In the AF solution of Dunlap,[55] these moments are localized on the atomic sites, but we find a lower-energy AF solution by localizing the moments on opposite sides of the bond axis. The singlet valence-electron spin densities are conceptually

$$\rho_\uparrow=\psi_{\pi_{ux}}^2+[A\psi_{\pi_{uy}}+B\psi_{\sigma_{gz}}]^2 , \tag{17}$$

$$\rho_\downarrow=\psi_{\pi_{ux}}^2+[A\psi_{\pi_{uy}}^2-B\psi_{\sigma_{gz}}]^2 , \tag{18}$$

where $A^2+B^2=1$. It is the AF singlet ($B\neq 0$) that we take to represent the ground state of the molecule in Table VI, even though it still lies about 0.2 eV above the triplet state in our density-functional calculations. This situation would probably be improved by PW GGA-IIA, which favors antiferromagnetic order over ferromagnetic. However, prediction of the wrong ground state might still persist as an interconfigurational or interterm error of continuum density-functional approximations.

We have also calculated the atomization energy of an isolated C_{60} (fullerene) molecule via LSD and PW GGA-II. Within LSD, we find a cohesive energy of 8.46 eV/atom.[56] Using basis sets of similar quality and the same exchange-correlation functional, Dunlap *et al.*[57] found a cohesive energy of 8.54 eV/atom. Within PW GGA-II, we find 7.38 eV/atom.[56] By performing PW GGA-II calculations with the same basis set on the similar C_6H_6 molecule and noting a 0.21 eV/carbon difference between the experimental and PW GGA-II cohesive energy, we estimate that the true cohesive energy of a static C_{60} molecule is closer to 7.25 eV. For comparison, we note that the measured enthalpy of formation of diamond (7.35 eV) and the theoretical zero-point vibrational energy (0.20 eV) due to Kong *et al.*[22] may be combined to estimate the cohesive energy of static diamond as 7.55 eV. This analysis suggests that the fullerene molecule is about 0.3 eV/atom less stable than diamond.

IV. SOLIDS

Solids, and especially metals, should be well suited to a continuum density-functional description based upon the electron gas of slowly varying density, for two reasons: (1) The reduced density gradients in the interior of a solid never get too large [e.g., the parameter s of Eq. (7) is never much greater than unity], and (2) the valence-electron orbitals of a solid form a continuum, as they do in the electron gas.

Although cohesive (atomization) energies of solids are overestimated by LSD, purely solid-state properties are often described very accurately. However, the zero-temperature ($T=0$) lattice constants of the alkali metals are a surprising exception to this rule: LSD underestimates the lattice constants of Li and Na by 3.2% and 4.1% (Table IX), in comparison with experiment.[58,59] While LSD typically underestimates the lattice constants of metals, its errors for the alkali metals are exceptionally large, despite the free-electron character of these metals. The error, which correlates with the compressibility of the metal, is greatest for Cs. (Our LSD lattice constants for Li and Na in Table IX agree with those of Sigalis *et al.*,[60] who considered all the alkali metals, but our value for bcc Li differs from that of an earlier LSD calculation.[61])

In order to investigate this problem, we have per-

TABLE IX. Cube-side lattice constant a, bulk modulus B, and structural energy difference per atom $E_{bcc}-E_{fcc}$ for solid Li and Na in the body-centered-cubic and face-centered-cubic structures. (1 bohr=0.529 177 Å; 1 hartree/bohr^3=29 420 GPa; 1 meV=10^{-3} eV.) LSD densities are employed for all calculations other than LM; the Langreth-Mehl (f=0.15) calculations are fully self-consistent. To within the accuracy of our numerical calculation (1%), the ratio of fcc to bcc volume per atom is unity for Li in all the approximations considered. Experimental values include the effect of zero-point vibration. The bulk modulus of Na was measured at T=78 K. (The experimental values of r_s are 3.24 and 3.93 bohrs for Li and Na, respectively.)

Property	Crystal	LSD[a]	LSD	LM	PW GGA-I	PW GGA-II	Expt.
a (bohr)	fcc Li	8.01	8.00	8.41	8.09	8.19	
	bcc Li	6.37	6.36	6.71	6.43	6.51	6.57[b]
	bcc Na	7.65	7.65	8.11	7.82	7.97	7.98[c]
B (GPa)	fcc Li	14.7	15.5	14.0	14.8	13.3	
	bcc Li	15.1	15.0	13.3	14.3	13.4	13.0[d]
	bcc Na	9.2	9.2	6.4	8.4	7.1	7.4[e]
$E_{bcc}-E_{fcc}$ (meV)	Li	6.4	4.2	2.7	3.9	3.7	

[a]Reference 60.
[b]Reference 58.
[c]Reference 59.
[d]Reference 64.
[e]Reference 66.

formed general-potential linearized-augmented-plane-wave[62] (LAPW) calculations (with relativistic cores) for Li and Na. Because the generalized gradient approximations (GGA's) are sensitive to nonspherical components of the density, we reject shape restrictions on the density or potential. The calculations presented here are highly converged, both with respect to basis-set size and Brillouin-zone sampling. (We used 60 and 112 special **k** points for the fcc and bcc structures, respectively.)

Unlike the calculations of Secs. II and III, some of our solid-state calculations achieve full self-consistency for each density functional considered: LSD, PW GGA-I, and PW GGA-II. (For Na, we tested the non-self-consistent procedure described in Sec. II and found that the results were unchanged within the numerical error of the calculation, 0.5% to 1% of the lattice constant. This procedure, which employs the LSD density, was implemented for Li as well.)

As shown in Table IX and in earlier studies,[20,21,24] GGA corrections to LSD increase the lattice constants of metals in the direction of experiment.[58,59] PW GGA-II underestimates the lattice constants of Li and Na by only 0.9% and 0.1%, respectively.

We now analyze the remaining small discrepancy between PW GGA-II theory and experiment for bcc Li. The experimental lattice constant[58] in Table IX was measured at T=20 K. Because the Li atom is so light, its low-temperature lattice constant must include a contribution from anharmonic zero-point vibration, which makes it larger than the static-lattice value we are trying to calculate. We might hope to eliminate this contribution by extrapolating the "classical" region of linear thermal expansion[63] ($200<T<300$ K) to T=0. The result is a bcc lattice constant of 6.54 bohr, only 0.5% larger than our PW GGA-II theoretical value. Alternatively, we could reduce the experimental value from Table IX by 0.6%, a theoretical estimate from Ref. 64, leaving a static-lattice constant only 0.3% bigger than our PW GGA-II theoretical value.

At low temperature, Li is a combination of body-centered-cubic (bcc) and close-packed 9R crystal structures. At T=78 K, the volume per atom is 142.5 bohr^3 for each phase.[65] The two phases appear to be close in energy, with 9R slightly lower. To simulate the 9R phase, we follow the lead of Sigalas *et al.*,[60] who performed calculations for the close-packed face-centered-cubic (fcc) structure of Li. As in Ref. 60, we find that the fcc energy per atom is slightly lower than the bcc energy. In the present well-converged calculations, a value of 0.004 eV is obtained for this difference. GGA corrections to LSD have little effect on this structural energy difference.

In Table IX we also report the bulk modulus B (inverse compressibility), in comparison with experiment.[64,66] At zero temperature, we calculate the pressure

$$P=-\partial E/\partial\Omega \tag{19}$$

and its derivative

$$B=-\Omega\partial P/\partial\Omega\ , \tag{20}$$

where E and Ω are the total energy per atom and volume per atom. The experimental values for cubic crystals are constructed from measured elastic constants[64,66] by the formula[67]

$$B=(C_{11}+2C_{12})/3\ . \tag{21}$$

Table IX shows that the LSD overestimation of the bulk modulus is largely corrected by PW GGA-II.

The observed ground state of metallic Fe is a ferromagnetic bcc lattice. The wrong ground state predicted by LSD (Ref. 68) (a paramagnetic fcc lattice) is corrected by PW GGA-I.[21,24] Our LAPW calculations show that PW GGA-II also predicts the true ground state for Fe.

Because the metals Pd and V are close to being fer-

romagnetic in LSD (i.e., they have large LSD spin-susceptibility enhancements[69] $\chi/\chi_0=4.5$ and 2.3, respectively), one might wonder if the GGA's would incorrectly tip these metals over into the ferromagnetic state. However, our LAPW calculations[70] at the experimental lattice constants show that these metals are correctly paramagnetic in the PW GGA-II approximation.

LSD fails to predict the observed insulating antiferromagnetic ground state for the high-temperature superconductor La_2CuO_4 and other layered cuprate materials such as $CaCuO_2$.[71] Singh and Pickett[25] have shown that $CaCuO_2$ is also incorrectly predicted to have a metallic paramagnetic ground state by the Langreth-Mehl (LM),[4,5] Becke,[10] and PW GGA-II functionals. By calculating a generalized inverse susceptibility, they found that the LM and PW GGA-II approximations at least bring $CaCuO_2$ closer to antiferromagnetism than do the LSD and Becke approximations.

V. SURFACES

The surfaces of metals should be amenable to a continuum density-functional description, since the valence-electron orbitals form a continuum. However, the divergence of the reduced density gradients s and t of Eqs. (7) and (10) far outside the metal poses a challenge to continuum approximations based upon the electron gas of slowly varying density, such as LSD and GGA. (See Figs. 2–4 of Ref. 72.)

The surface properties we consider are the work function W, surface energy σ, and curvature energy γ. The work function is simultaneously the ionization energy, electron affinity, and electronegativity of the metallic crystal. The surface and curvature energies enter the liquid-drop expansion for the total energy of an extended system with volume V and surface area A:

$$E=\alpha V+\sigma A+\tfrac{1}{2}\gamma\int dA\ \mathcal{R}^{-1}\ , \tag{22}$$

where $\mathcal{R}^{-1}$ is the mean curvature of area element dA.

Since these surface properties for the simple metals are determined largely by the bulk valence-electron density

$$\bar{\rho}=3/4\pi r_s^3\ , \tag{23}$$

we study two models characterized only by the bulk density parameter r_s, viz., jellium and stabilized jellium.[73,74] In jellium, the electrons are bound to a positive background of uniform density which vanishes outside a sharp surface. But jellium is stable only at $r_s=4.2$ bohr. In *stabilized* jellium, the electrons interact with an additional short-range potential, chosen to make the bulk stable at a given r_s. This additional potential is constant inside the sharp surface, and vanishes outside. Especially for the simple high-density metals ($r_s\approx 2$, where the jellium surface energy is negative), stabilized jellium is the more realistic model. We evaluate W, σ, and γ from Kohn-Sham calculations for the planar surface, as in Refs. 75 and 76.

We begin with the infinite barrier model of the jellium surface, in which the Kohn-Sham potential is replaced by an infinite step. For this non-self-consistent model, the surface energies are known within the random-phase approximation (RPA).[77,78] We easily construct RPA versions of LSD and PW GGA-II, using RPA input for $\varepsilon_c(r_s,\zeta)$ (Ref. 26) and $C_c(r_s)$ (Ref. 3) in Eq. (1) or (9). Table X shows that LSD seriously underestimates the correlation contribution σ_c to the surface energy, while PW GGA-II fortuitously yields the exact σ_c, to the accuracy with which it is known. For the surface exchange energy σ_x, the situation is less satisfactory. While LSD overestimates σ_x by 55%, a direct calculation of σ_x (PW GGA-II) underestimates σ_x by 36%. This underestimation is more severe for PW GGA-I (44%) and for Becke[10] (57%) and Vosko-Macdonald[9] (62%) exchange. However, as Table X shows, the quantity

$$\sigma_x'(\text{PW GGA-II})\equiv\sigma_x(\text{PW GGA-II})+(2315\ \text{erg/cm}^2)/r_s^3 \tag{24}$$

TABLE X. Surface exchange energy σ_x and correlation energy σ_c (within the random-phase approximation) for the infinite-barrier model of the jellium surface. r_s is the bulk density parameter. (1 hartree/bohr$^2=1.556\,92\times10^6$ erg/cm^2.) PW GGA-II values include the long-range correction of Eq. (24). Exact values from Ref. 77, as corrected in Ref. 78. Note that the Langreth-Mehl approximation (LM, $f=0.17$) breaks down for this rapidly varying density profile, but still works well for the more physical profiles of Tables XI and XII.

		Infinite-barrier model (erg/cm^2)			
Component	r_s	LSD	LM	PW GGA-II	Exact
σ_x	2.07	1109	−1396	715	715
	4	154	−194	99	99
	6	46	−57	29	29
σ_c^{RPA}	2.07	136	1498	648	673
	4	31	239	117	104
	6	12	78	40	34
σ_{xc}^{RPA}	2.07	1245	102	1363	1388
	4	185	45	216	203
	6	58	21	70	63

TABLE XI. Surface exchange energy σ_x and correlation energy σ_c for jellium, with self-consistent density profiles. PW GGA-II surface energies include the long-range contribution from Eq. (24). The difference between exact and LSD values for σ_x is estimated from Tables VI and VII of Ref. 12.

	σ_x (erg/cm^2)			σ_c (erg/cm^2)		$\sigma_{xc}=\sigma_x+\sigma_c$	
r_s	LSD	PW GGA-II	Exact	LSD	PW GGA-II	LSD	PW GGA-II
2.07	2670	2306	2309	293	746	2963	3052
3.99	225	156	164	39	123	264	279
5.63	57	29	36	13	47	70	76

reproduces the exact σ_x. We regard the second term on the right of Eq. (24) as a radically nonlocal contribution arising from long-range density fluctuations neglected in PW GGA-II. It is perhaps only for a semi-infinite system (and not for atoms, molecules, or bulk solids near equilibrium) that the exact exchange-correlation hole has a long-ranged tail[78,79] and so cannot be modeled reliably by the finite-ranged PW GGA-II hole. The correction to the surface exchange-correlation energy from this long-range tail is necessarily positive. That the needed correction to σ_{xc} is smaller for LSD (about [1270 erg/cm^2]/r_s^3) than for PW GGA-II is probably accidental.

A better-justified correction to the PW GGA-II surface energy would replace the separate radial cutoffs on the exchange and correlation holes by a single radial cutoff on their sum, and would further replace the zero hole density outside this radius by the known long-range tail. In future work, we hope to construct this real-space GGA analog of the Langreth-Perdew wave-vector interpolation.[78]

Now we turn to self-consistent surface density profiles (Tables XI and XII). As for the infinite-barrier model, the long-range correction of Eq. (24) brings the PW GGA-II surface exchange energies into agreement with exact values[12] (although this correction is now a smaller fraction of σ_x). We expect that the PW GGA-II surface correlation energies are still correct, since (a) the self-consistent profiles are more slowly varying than the infinite-barrier profiles and (b) corrections to the RPA have no long-range contribution. From Table XII and Eq. (24), it is clear that the PW GGA-II work functions W, surface energies σ (neglecting the long-range part), and curvature energies γ are all slightly lower than the corresponding LSD values. In Sec. VI we will relate this PW GGA-II reduction in σ and γ to the PW GGA-II reduction of atomic total energy found in Sec. II and the PW GGA-II reduction of atomization energy found in Sec. III. When the long-range contribution of Eq. (24) is included (as it has been in Tables XI and XII), the PW GGA-II surface energies are slightly higher than LSD values.

The PW GGA-II surface energies for self-consistent jellium profiles (Table XII) are in good agreement with Langreth-Mehl values[80] (for which no long-range correction is invoked) and also with the result of the Green's-function quantum Monte Carlo method[81] ($\sigma=-470$ erg/cm^2 for $r_s=2.07$). Moreover, the PW GGA-II work function, surface energy, and curvature energy for *stabilized* jellium are in reasonable agreement with experimental values for the real metals.[82–84] (A more general but also more demanding approach to metallic surfaces or clusters would combine an exact description of exchange

TABLE XII. Work function W, intrinsic (ideally flat) surface energy σ, and curvature energy γ for jellium and stabilized jellium, with self-consistent density profiles. (1 millihartree $=10^{-3}$ hartree.) PW GGA-II surface energies include the long-range contribution from Eq. (24). Langreth-Mehl (LM, $f=0.17$) values from Ref. 80. For comparison, experimental or phenomenological values are presented for the *real* metals Al ($r_s=2.07$), Na ($r_s=3.99$), and Cs ($r_s=5.63$). The experimental work function is the polycrystalline value (Ref. 82). The "experimental" value for the intrinsic surface energy is the zero-temperature extrapolation of the liquid-metal surface tension (Ref. 83), divided by the corrugation factor of 1.2 (Ref. 84). The "experimental" curvature energy is obtained from the measured vacancy-formation energy ε_{vac} by the liquid-drop equation $\gamma=[\sigma 4\pi r_0^2-\varepsilon_{vac}]/2\pi r_0$, as in Ref. 84, but with the long-range contribution of Eq. (24) subtracted from the experimental surface energy σ (consistent with the approach of Table XIII).

		Jellium			Stabilized jellium		
Property	r_s	LSD	LM	PW GGA-II	LSD	PW GGA-II	Expt.
W (eV)	2.07	3.74	4.12	3.65	4.24	4.17	4.28
	3.99	2.91	3.32	2.88	2.92	2.90	2.75
	5.63	2.35	2.74	2.30	2.24	2.23	2.14
σ (erg/cm^2)	2.07	−605	−484	−473	953	1060	953
	3.99	164	189	185	171	191	218
	5.63	71	82	80	60	69	79
γ (millihartree/bohr)	2.07	1.77		1.47	1.82	1.50	1.35
	3.99	0.36		0.31	0.35	0.30	0.28
	5.63	0.13		0.11	0.13	0.12	0.19

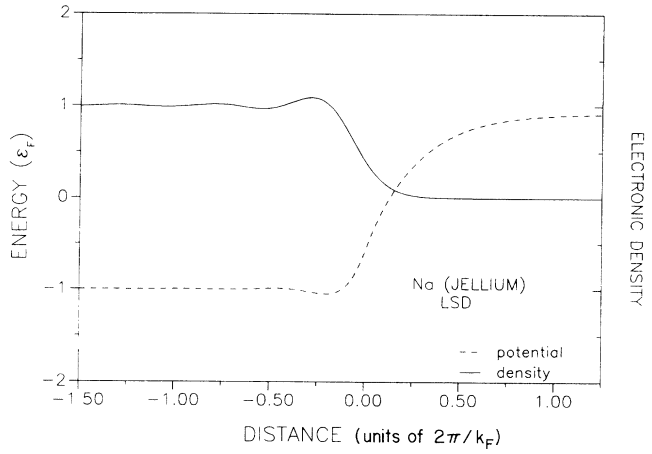

FIG. 1. LSD solution for the $r_s=3.99$ jellium surface. The solid curve is the electron-density profile, measured in units of the bulk density $k_F^3/3\pi^2$. The dashed curve is the self-consistent one-electron potential, measured in units of the bulk Fermi energy $k_F^2/2$. A constant has been added to this potential to make it tend to $-k_F^2/2$ in the bulk. Distance from the jellium edge is measured in units of the Fermi wavelength $2\pi/k_F$.

with PW GGA-II correlation.)

The correction that we find to the LSD surface energy is rather small, as a result of a delicate cancellation between the nonlocalities of exchange and correlation (Tables X–XII). This correction is much smaller than that found by the Fermi hypernetted-chain method,[85] which was regarded as the standard before the advent of the quantum Monte Carlo calculation.[81] However, it is consistent with the results of Skriver and Rosengaard,[86] who calculated LSD surface energies, for the close-packed faces of the alkali metals, that agree closely with measured liquid-metal surface tensions extrapolated to zero temperature. Note further that a sophisticated version of the fully nonlocal weighted-density approximation gives surface energies close to those of LSD.[87]

The LSD and PW GGA-II electron-density profiles

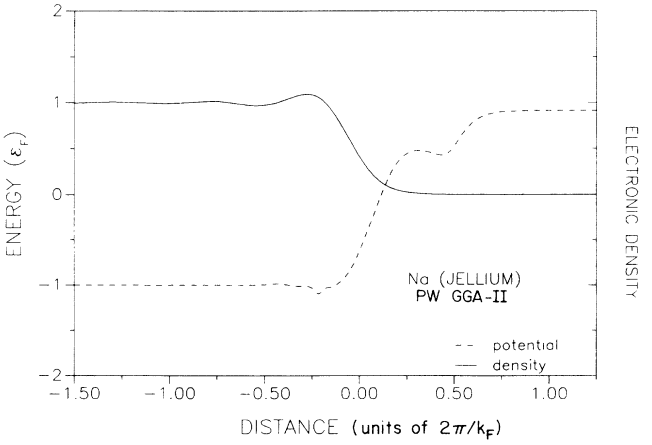

FIG. 2. PW GGA-II solution for the $r_s=3.99$ jellium surface. See caption of Fig. 1.

and one-electron potentials for the $r_s=3.99$ jellium surface are displayed in Figs. 1 and 2. On the scale of these figures, the LSD and PW GGA-II density profiles are indistinguishable. The potentials are barely distinguishable until the electron density has decayed to about 10% of its bulk value. From this point, the PW GGA-II potential first rises above and then dips below the LSD potential. A similar oscillation is found in the PW GGA-I and LM potentials for atoms.[19]

VI. ATOMS, SOLIDS, AND SURFACES IN THE JELLIUM MODEL: A UNIFIED PERSPECTIVE

Here we present simple estimates which tie together our results for atomic total energies (Sec. II), atomization energies (Sec. III), and surface and curvature energies (Sec. V). Use will be made of the jellium model of Sec. V.

According to the liquid-drop model for crystalline metals,[84] the expansion (22) can be valid even for microscopic radii of curvature, so long as electronic shell-structure effects may be neglected. Clear-cut examples are provided by the monovacancy-formation energy and the crystal-face dependence of the surface energy for a metal of infinite volume. The expansion (22) also seems to apply to one-electron atoms, i.e., the shell-structure oscillation tends to vanish for these systems with half-filled shells.

Consider a monovalent atom of jellium, i.e., one electron bound to a uniform positive background of density $3/4\pi r_s^3$ confined inside a sharp spherical surface of radius r_s. The total energy is[88] $-I+3/5r_s$, where I is the energy needed to ionize the electron and $3/5r_s$ is the electrostatic energy of the positive background. Since this is a one-electron problem, I is easily calculated exactly or in a density-functional approximation.[88]

The cohesive energy of jellium is the atomization energy per atom, i.e.,

$$\varepsilon_{\rm coh}=[-I+3/5r_s]-\varepsilon\ , \tag{25}$$

where $\varepsilon=3k_F^2/10+\varepsilon_{\rm xc}(r_s)$ is the energy per electron in the uniform or condensed phase. By Eq. (22), the liquid-drop-model estimate of the cohesive energy[84] is just the energy needed to create the curved surface of the jellium atom:

$$\sigma 4\pi r_s^2+\gamma 2\pi r_s\ . \tag{26}$$

In Table XIII we compare the LSD cohesive energy of Eq. (25) against the liquid-drop prediction of Eq. (26), using LSD values for σ and γ from Sec. V. We also compare the exact cohesive energy against the liquid-drop prediction, using PW GGA-II values for σ and γ. [We omit the long-range contribution of Eq. (24), which arises from an effect present only for a semi-infinite system and thus irrelevant to the cohesive energy.] The following conclusions may be drawn: (1) Except at the highest density considered ($r_s=2.07$), the liquid-drop model has good quantitative accuracy. Even at $r_s=2.07$, the curvature term helps. (The liquid-drop model must fail in the limit $r_s\to 0$, in which the jellium atom reduces to hydro-

TABLE XIII. Prediction of the liquid-drop model [Eq. (26)] compared with the cohesive energy of Eq. (25) for jellium with bulk density parameter r_s. The first three rows employ LSD values for the surface, curvature, and cohesive energies. The last three rows employ PW GGA-II values for the surface and curvature energies, and exact (not density-functional) values for the cohesive energies. Here the PW GGA-II surface energies do *not* include the long-range contribution of Eq. (24). The LSD energy for the monovalent jellium atom was calculated with the exact one-electron density. The last column is the liquid-drop-model cohesive energy for *stabilized* jellium.

Method	r_s	Cohesive energy of jellium (eV) $\sigma 4\pi r_s^2$	$\sigma 4\pi r_s^2+\gamma 2\pi r_s$	ε_{coh}	Stabilized $\sigma 4\pi r_s^2+\gamma 2\pi r_s$
LSD	2.07	−0.57	0.06	0.48	1.54
	3.99	0.57	0.82	0.88	0.84
	5.63	0.49	0.62	0.63	0.54
PW GGA-II	2.07	−0.69	−0.17	0.24	1.28
	3.99	0.52	0.73	0.77	0.75
	5.63	0.47	0.57	0.57	0.51

gen.) (2) LSD cohesive energies are higher than exact ones. Thus LSD overestimates the atomization energy for jellium, as it does for molecules and real solids. (3) Since the bulk of jellium is uniform, LSD yields the exact bulk energy. Therefore, LSD overestimates the total energy of a jellium atom, as it does for a real atom. (4) Since the surface and curvature energies are lower in PW GGA-II than in LSD, the PW GGA-II atomization and total energies are also lower and thus closer to the exact values. Table XIII suggests that, in comparison with LSD, PW GGA-II gives a better description of the contribution to σ and γ from intermediate-range density fluctuations. (Long-range fluctuations are essentially absent from one-electron atoms.)

As first shown by Kutzler and Painter,[14] GGA's favor nonspherical densities more than LSD does (cf. our discussion of the carbon atom in Sec. III). From the liquid-drop model, the same effect may be expected for jellium. Consider a volume-conserving oblate or prolate spheroidal distortion of the one-electron jellium atom, which increases the area and the curvature integral of Eq. (22).[89] Since the PW GGA-II functional predicts lower values for σ and γ, it penalizes this distortion less severely than LSD does.

For these one-electron atoms (as for the hydrogen atom or the systems of Table VI), PW GGA-II may be regarded as an approximate self-interaction correction[39] to LSD. More generally, PW GGA-II contains information about real electron-electron interactions in inhomogeneous systems, as the bulk-metal results of Sec. IV demonstrate.

The importance of exchange and correlation for valence electrons in general, and for jellium in particular, cannot be overemphasized. Without exchange and correlation, bulk jellium would be unstable (or at least unrealistic) in several ways: (1) The pressure of Eq. (19) would not vanish at any finite r_s, and (2) the surface, curvature, and atomization energies would be either negative or absurdly small at all r_s, as would the work function.[50,76]

These instabilities are removed in the following way: (1) Creation of the exchange-correlation hole around each electron lowers the bulk energy per electron by an amount roughly proportional to r_s^{-1}, and so opposes the expansion driven by the kinetic energy (which raises the energy per electron by an amount proportional to r_s^{-2}). (2) An electron which penetrates into the surface region gets partially separated from its exchange-correlation hole (which lags behind in a region of higher density), and this effect raises the surface energy. Because the separation is more complete for a convex ($\mathcal{R}^{-1}>0$) surface than for a concave ($\mathcal{R}^{-1}<0$) one, the same effect also raises the curvature energy. In order to remove an electron completely, positive work must be done to separate it from its exchange-correlation hole.[90]

VII. UNDERSTANDING NONLOCALITY

In order to visualize the nonlocality of PW GGA-II exchange and correlation [Eqs. (3)–(15)], we define an enhancement factor F_{xc} (relative to spin-unpolarized local exchange). For the case of uniform ζ ($\nabla\zeta=0$), we write

$$E_{xc}^{\text{PW GGA-II}}[n_\uparrow,n_\downarrow]=\int d^3r\, n\varepsilon_x(r_s,0)F_{xc}(r_s,\zeta,s)\ , \qquad (27)$$

where s is the reduced density gradient of Eq. (7). We note that the reduced gradient of Eq. (10) is

$$t=1.228s/\sqrt{r_s}g(\zeta)\ . \qquad (28)$$

Figures 3 and 4 display F_{xc} for the spin-unpolarized ($\zeta=0$) and fully polarized ($\zeta=1$) cases, respectively. From the viewpoint of Slater's $X\alpha$ method,[91] F_{xc} provides a position-dependent $\alpha=\frac{2}{3}F_{xc}$.

The nonlocality is borne by the s dependence of F_{xc}. In fact, the LSD approximation replaces $F_{xc}(r_s,\zeta,s)$ by

$$F_{xc}(r_s,\zeta,0)=\varepsilon_{xc}(r_s,\zeta)/\varepsilon_x(r_s,0)\ ,$$

i.e., by horizontal straight lines not shown in Figs. 3 and 4. Although it is not evident on the scale of these figures, the PW GGA-II curve for each r_s starts out from $s=0$ with a negative second derivative. Thus the ungeneralized second-order gradient expansion replaces $F_{xc}(r_s,\zeta,s)$ by a downward-turning parabola

$$F_{xc}(r_s,\zeta,0)-|C(r_s,\zeta)|s^2\ .$$

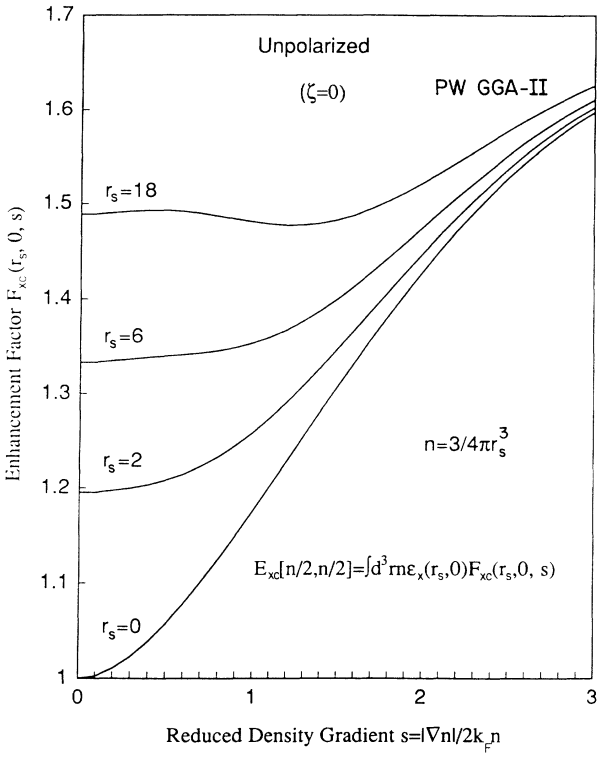

FIG. 3. PW GGA-II nonlocality in the spin-unpolarized case. The enhancement factor $F_{xc}(r_s,0,s)$ (relative to spin-unpolarized local exchange) is plotted vs the reduced density gradient s for several values of the local-density parameter r_s. The corresponding enhancement factors for LSD are the horizontal lines $F_{xc}(r_s,0,0)=\varepsilon_{xc}(r_s,0)/\varepsilon_x(r_s,0)$. For the second-order gradient expansion, they are downward-turning parabolas $F_{xc}(r_s,0,0)-|C(r_s,0)|s^2$.

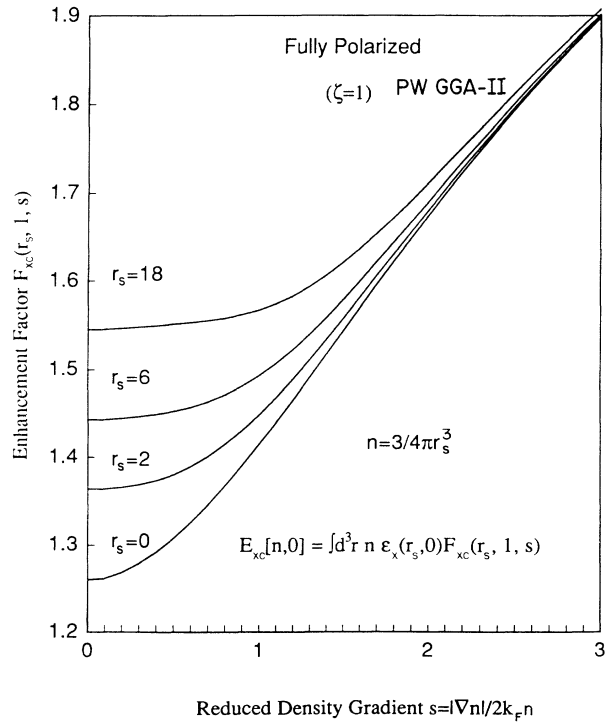

FIG. 4. Same as Fig. 3, but for the fully spin-polarized case.

The values of s that are important in the interior of a metal typically fall in the range $0 \lesssim s \lesssim 2.0$. Atoms sample the range $0.2 \lesssim s$, with s diverging into the vacuum around the atom.[72] (Within an electronic shell, $|\nabla n|/n$ is approximately constant, but k_F^{-1} and s increase in the outward direction.) Clearly, for most physical properties of real systems, the nonlocal effect of PW GGA-II is *opposite* to that of the second-order gradient expansion. Thus, Bagno, Jepsen and Gunnarsson[21] found that the gradient expansion shrinks the lattice constants of metals, which are already too small in LSD, and further destabilizes the bcc ferromagnetic ground state of Fe, which is wrongly unstable in LSD. PW GGA-II has the opposite (and correct) effects.

The exchange-only PW GGA-IIX nonlocality is presented in the $r_s=0$ curves of Figs. 3 and 4. The nonlocality of exchange ($E_x^{\text{PW GGA-II}} < E_x^{\text{LSD}} < 0$), which favors density inhomogeneity, is strong when s is of order unity, i.e., when the density varies significantly over the range of the exchange hole. An opposite nonlocality ($0 > E_c^{\text{PW GGA-II}} > E_c^{\text{LSD}}$), which opposes density inhomogeneity, extinguishes the correlation contribution to F_{xc} as $t \to \infty$. (Compare the similar behavior of the linear response function in Ref. 41, and the somewhat different behavior produced by the wave-vector-space cutoff of Refs. 4 or 8.) In the high-density limit ($r_s \to 0$), the correlation contribution vanishes on the scale of these figures. But for metallic densities ($2 \lesssim r_s \lesssim 6$), the nonlocality of correlation cancels much of that for exchange ($E_{xc}^{\text{PW GGA-II}} \lesssim E_{xc}^{\text{LSD}}$). For these and lower densities, the exchange-correlation hole is significantly deeper and (apart from oscillations) more short ranged than the exchange hole, making F_{xc} larger and more "local" than F_x. As a result, LSD can give a reasonably good description of valence-electron energies in metals, even though it makes serious errors for the cores.

Since the residue of this cancellation between nonlocalities is still exchangelike in PW GGA-II, the principal PW GGA-II nonlocal effect is to favor density inhomogeneity or surface formation more than LSD does. Thus the PW GGA-II correction to LSD lowers total, atomization, surface, and curvature energies. It enlarges the lattice constants of metals, where expansion continuously increases the inhomogeneity. PW GGA-II also favors nonspherical distortions over spherical densities.

Although the PW GGA-II functional improves upon LSD, too much should not be expected from it:

(1) Even the exact density functional would not predict all excited-state energies,[1,2] nor would its Kohn-Sham eigenvalue spectrum predict the fundamental gap (twice "hardness") of an insulator or semiconductor[28,29] or the exact Fermi surface of a metal.[92]

(2) Many incorrect features of LSD are carried over into PW GGA-II and other GGA's: (a) Incorrect asymptotic decay[30,39] of the density and one-electron potential into the vacuum, blocking self-consistent solutions for negative ions; (b) absence of derivative discontinuities, leading to incorrect fractionally charged fragments instead of neutral atoms as dissociation products of heteronuclear molecules or solids;[28,29] (c) interconfigurational and interterm errors of ionization energies and

electron affinities (Sec. II); and (d) symmetry[55] and multiplet problems.[93,94] These incorrect features should be least troubling in bulk simple metals, or perhaps in solids under pressure.

VIII. CONCLUSIONS

In a variety of tests for atoms, molecules, solids, and surfaces, we have found that the Perdew-Wang generalized gradient approximation (PW GGA-II) for exchange and correlation is usually more accurate than the local-spin-density (LSD) approximation or older GGA's. Many of the PW GGA-II nonlocal effects have a simple qualitative explanation (Sec. VII).

Unlike LSD, PW GGA-II total energies of atoms are highly accurate. Atomic ionization energies and electron affinities display the interconfigurational and interterm errors that are apparently common to LSD and all GGA's (at least within the central-field approximation for the potential), but the root-mean-square error is slightly reduced by PW GGA-II. The best accuracy is achieved by (a) applying PW GGA-II to realistic Hartree-Fock densities and (b) considering only processes free from interconfigurational and interterm error (e.g., removal of two valence s electrons).

PW GGA-II atomization energies are also highly accurate. For seven hydrocarbon molecules with LSD densities and geometries, PW GGA-II achieves a rms error of 0.1 eV per bond, compared to 0.7 eV per bond for LSD and 2.4 eV per bond for Hartree-Fock theory. Buckminsterfullerene (C_{60}) is predicted to be about 0.3 eV/atom less stable than diamond. Numerical results for a much larger class of molecules[95] are also encouraging.

For both atoms and molecules, there is a cancellation of error between density functionals for exchange and correlation, which should therefore be treated together in the same way. This error cancellation is most striking whenever Hartree-Fock is a poor zero-order approximation (e.g., the electron affinity of N and the atomization energy of C_2).

Good results are also found for solids. While LSD underestimates the lattice constants of Li and Na by 3.2% and 4.1%, respectively, PW GGA-II reduces the underestimation to less than 1%. This increase in theoretical lattice constant is accompanied by an improvement in the bulk modulus.

Of all natural systems, bulk simple metals should be most amendable to a generalized gradient approximation based upon the electron gas of slowly varying density. Thus the agreement between PW GGA-II theory and precise measurements of the lattice constants for Li and Na is especially significant. Metals are also the physical systems that should be best suited to the *ungeneralized* second-order gradient expansion of the exchange-correlation energy, which, however, underestimates their lattice constants even more severely than LSD does.[21] Because of the long range of the Coulomb interaction between electrons, the ungeneralized expansion appears to be valid only in an unphysical limit of slowly varying density, as originally asserted in Refs. 3 and 78. (This conclusion is antithetical to that of Ref. 40.)

When LSD predicts the true ground state (e.g., solid Pd), PW GGA-II tends to do the same. In some cases (e.g., the molecule C_2 and the solid $CaCuO_2$), both LSD and PW GGA-II predict the wrong ground state. In other cases (e.g., solid Fe), the wrong LSD ground state is corrected by PW GGA-II.

For metal surfaces, the work function, surface energy, and curvature energy are all slightly lower in PW GGA-II than in LSD. For the separate exchange and correlation components of the surface energy, PW GGA-II is more accurate than LSD. However, neither LSD nor PW GGA-II includes the contribution to the surface energy from long-range density fluctuations [which must therefore be added by hand, as in Eq. (24)]. Via the liquid-drop model, the reduced surface and curvature energies of PW GGA-II "explain" why atomic total energies and atomization energies are lower in PW GGA-II than in LSD.

While more extensive tests are needed, we tentatively recommend the PW GGA-II generalized gradient approximation for problems requiring better accuracy than LSD for a modest increase of computation. We also stress that the improvement over LSD is attributable to the nonspurious part of the gradient expansion.

Fully nonlocal alternatives to GGA's, such as self-interaction corrections[39] or weighted-density approximations,[34,87,96] are considerably harder to implement, especially for large systems. These fully nonlocal approximations typically have better asymptotic behavior of the atomic potential, but GGA's might be expected to give a better description of ground-state properties for bulk solids, especially the simple metals.

In principle, neither LSD nor PW GGA-II can describe the long-range part of the exchange-correlation hole. Fortunately, this does not seem to be an important limitation for most properties of interest in condensed-matter physics and quantum chemistry. For the metal surface energy, however, the exceptionally long-ranged tail of the exchange-correlation hole[79] must be taken into account exactly or via Eq. (24).

ACKNOWLEDGMENTS

One of us (J.P.P.) acknowledges discussions with Mel Levy, assistance from Yue Wang, and the hospitality of the Complex Systems Theory Branch of the Naval Research Laboratory (where part of this work was done). Partial support from the National Science Foundation under Grant No. DMR 88-17866 (J.P.P.) and the Natural Sciences and Engineering Research Council of Canada under Grant No. OGP0006244 (J.A.C. and S.H.V.) is gratefully acknowledged. Work at the Naval Research Laboratory is supported by the Office of Naval Research. Some computations were performed at the Cornell National Supercomputer Facility.

[1]W. Kohn and L. J. Sham, Phys. Rev. **140**, A1133 (1965).
[2]R. O. Jones and O. Gunnarsson, Rev. Mod. Phys. **61**, 689 (1989).
[3]D. C. Langreth and J. P. Perdew, Phys. Rev. B **21**, 5469 (1980).
[4]D. C. Langreth and M. J. Mehl, Phys. Rev. B **28**, 1809 (1983).
[5]C. D. Hu and D. C. Langreth, Phys. Scr. **32**, 391 (1985).
[6]J. P. Perdew, Phys. Rev. Lett. **55**, 1665 (1985).
[7]J. P. Perdew and Y. Wang, Phys. Rev. B **33**, 8800 (1986).
[8]J. P. Perdew, Phys. Rev. B **33**, 8822 (1986); **34**, 7406(E) (1986).
[9]S. H. Vosko and L. D. Macdonald, in *Condensed Matter Theories,* edited by P. Vashishta, R. K. Kalia, and R. F. Bishop (Plenum, New York, 1987), Vol. 2.
[10]A. D. Becke, Phys. Rev. A **38**, 3098 (1988).
[11]J. B. Lagowski and S. H. Vosko, J. Phys. B **21**, 203 (1988).
[12]J. P. Perdew, M. K. Harbola, and V. Sahni, in *Condensed Matter Theories,* edited by J. S. Arponen, R. F. Bishop, and M. Manninen (Plenum, New York, 1988), Vol. 3.
[13]F. W. Kutzler and G. S. Painter, Phys. Rev. B **43**, 6865 (1991).
[14]F. W. Kutzler and G. S. Painter, Phys. Rev. Lett. **59**, 1285 (1987).
[15]F. W. Kutzler and G. S. Painter, Phys. Rev. B **37**, 2850 (1988).
[16]E. Clementi and S. J. Chakravorty, J. Chem. Phys. **93**, 2591 (1990); A. Savin, H. Stoll, and H. Preuss, Theor. Chim. Acta **70**, 407 (1986).
[17]P. Mlynarski and D. R. Salahub, Phys. Rev. B **43**, 1399 (1991).
[18]L. Fan and T. Ziegler, J. Chem. Phys. **94**, 6057 (1991).
[19]G. Ortiz and P. Ballone, Phys. Rev. B **43**, 6376 (1991).
[20]K. Kobayashi, N. Kurita, H. Kumahora, and K. Tago, Phys. Rev. A **43**, 5810 (1991).
[21]P. Bagno, O. Jepsen, and O. Gunnarsson, Phys. Rev. B **40**, 1997 (1989).
[22]X. J. Kong, C. T. Chan, K. M. Ho, and Y. Y. Ye, Phys. Rev. B **42**, 9357 (1990).
[23]R. Orlando, R. Dovesi, C. Roetti, and V. R. Saunders, J. Phys. Condens. Matter **2**, 7769 (1990).
[24]D. J. Singh, W. E. Pickett, and H. Krakauer, Phys. Rev. B **43** 11 628 (1991).
[25]D. J. Singh and W. E. Pickett, Phys. Rev. B **44**, 7715 (1991).
[26]J. P. Perdew and Y. Wang (unpublished). In this derivation, summarized in Ref. 27, extensive use is made of the high-density and long-range scaling properties of the correlation hole for a spin-polarized uniform electron gas, as discussed by Y. Wang and J. P. Perdew, Phys. Rev. B **44**, 13 298 (1991), and Ref. 42. J. P. Perdew and Y. Wang [Phys. Rev. B **45**, 13 244 (1992)] have constructed the analytic representation of the uniform-gas correlation energy used in this work. M. Levy and J. P. Perdew (unpublished) have tested PW GGA-II and other density functionals against a number of exact scaling relations, inequalities, and bounds.
[27]J. P. Perdew, in *Electronic Structure of Solids '91,* edited by P. Ziesche and H. Eschrig (Akademie Verlag, Berlin, 1991). A preliminary derivation for the high-density limit was given by J. P. Perdew, Physica B **172**, 1 (1991).
[28]J. P. Perdew, R. G. Parr, M. Levy, and J. L. Balduz, Jr., Phys. Rev. Lett. **49**, 1691 (1982). For a more detailed discussion of the band-gap problem, see J. P. Perdew and M. Levy, Phys. Rev. Lett. **51**, 1884 (1983); L. J. Sham and M. Schlüter, *ibid.* **51**, 1888 (1983).
[29]J. P. Perdew, in *Density Functional Methods in Physics,* edited by R. M. Dreizler and J. da Providência (Plenum, New York, 1985).
[30]J. B. Krieger, Y. Li, and G. J. Iafrate, Phys. Lett. A **146**, 256 (1990).
[31]J. P. Perdew, in *Condensed Matter Theories,* edited by P. Vashishta, R. K. Kalia, and R. F. Bishop (Plenum, New York, 1987), Vol. 2.
[32]Y. Wang, J. P. Perdew, J. A. Chevary, L. D. Macdonald, and S. H. Vosko, Phys. Rev. A **41**, 78 (1990).
[33]M. Slamet and V. Sahni, Int. J. Quantum Chem. S **25**, 235 (1991); Phys. Rev. B **44**, 10 921 (1991).
[34]J. A. Alonso and L. A. Girifalco, Phys. Rev. B **17**, 3735 (1978).
[35]D. R. Murphy and W.-P. Wang, J. Chem. Phys. B **72**, 429 (1980); G. L. Oliver and J. P. Perdew, Phys. Rev. A **20**, 397 (1979).
[36]E. Engel and R. M. Dreizler, J. Phys. B **22**, 1901 (1989).
[37]Two possible values for the exchange-only gradient coefficient were presented by L. J. Sham, in *Computational Methods in Band Theory,* edited by P. M. Marcus, J. F. Janak, and A. R. Williams (Plenum, New York, 1971), p. 458: One based upon an analytic treatment of a statically screened Coulomb interaction with the screening going to zero, and a second from an analysis of the numerical results of D. J. W. Geldart and R. Taylor, Can. J. Phys. **48**, 155 (1970). The first or analytic value is referred to as the Sham value C_x. The possibility that the second ($10C_x/7$) is the correct coefficient was raised by P. R. Antoniewicz and L. Kleinman, Phys. Rev. B **31**, 6779 (1985). Accurate numerical calculations by L. Kleinman and S. Lee, Phys. Rev. B **37**, 4634 (1988), and by J. A. Chevary and S. H. Vosko, *ibid.* **42**, 5320 (1990), showed that the second value was the correct one.
[38]S. H. Vosko, L. Wilk, and M. Nusair, Can. J. Phys. **58**, 1200 (1980).
[39]J. P. Perdew and A. Zunger, Phys. Rev. B **23**, 5048 (1981).
[40]M. Rasolt and D. J. W. Geldart, Phys. Rev. B **34**, 1325 (1986).
[41]D. C. Langreth and S. H. Vosko, Adv. Quantum Chem. **21**, 175 (1990); D. C. Langreth and J. P. Perdew (unpublished).
[42]Y. Wang and J. P. Perdew, Phys. Rev. B **43**, 8911 (1991).
[43]M. Rasolt and H. L. Davis, Phys. Lett. A **86**, 45 (1981).
[44]C. E. Moore, in *Atomic Energy Levels,* Natl. Bur. Stand. (U.S.) Circ. No. 467 (U.S. GPO, Washington, DC, 1970).
[45]H. Hotop and W. C. Lineberger, J. Phys. Chem. Ref. Data **14**, 731 (1985).
[46]V. Tschinke and T. Ziegler, J. Chem. Phys. **93**, 8051 (1990). See also Refs. 78 and 79.
[47]R. G. Parr and R. G. Pearson, J. Am. Chem. Soc. **105**, 7513 (1983).
[48]E. C. M. Chen, W. E. Wentworth, and J. A. Ayala, J. Chem. Phys. **67**, 2642 (1977).
[49]R. Monnier, J. P. Perdew, D. C. Langreth, and J. W. Wilkins, Phys. Rev. B **18**, 656 (1978).
[50]J. P. Perdew, Phys. Rev. B **21**, 869 (1980).
[51]M. R. Pederson, K. A. Jackson, and W. E. Pickett, Phys. Rev. B **44**, 3891 (1991). The LSD and GGA atomization energies reported in this reference employ *spherically averaged* atomic densities and small basis sets.
[52]M. R. Pederson and K. A. Jackson, Phys. Rev. B **41**, 7453 (1990).
[53]E. Hirota, S. Saito, and Y. Endo, J. Chem. Phys. **71**, 1183 (1979).
[54]K. P. Huber and G. Herzberg, *Molecular Structure and Molecular Spectra IV: Constants of Diatomic Molecules* (Van Nostrand Reinhold, New York, 1970).
[55]B. I. Dunlap, Adv. Chem. Phys. **69**, 287 (1987).
[56]M. R. Pederson (unpublished).
[57]B. I. Dunlap, D. W. Brenner, J. W. Mintmire, R. C. Mowrey, and C. T. White, J. Phys. Chem. **95**, 5763 (1991).
[58]R. Berliner and S. A. Werner, Phys. Rev. B **34**, 3586 (1986).

[59]W. B. Pearson, *A Handbook of Lattice Spacings and Structures of Metals and Alloys* (Pergamon, New York, 1967).

[60]M. Sigalis, N. C. Bacalis, D. A. Papaconstantopoulos, M. J. Mehl, and A. C. Switendick, Phys. Rev. B **42**, 11 637 (1990). These LSD calculations employ the Moruzzi-Janak-Williams (MJW) parametrization of ε_c. Because the MJW $\varepsilon_c(r_s,0)$ differs from more accurate parametrizations (Refs. 26, 38, and 39) by a nearly constant 0.10 eV over the range of metallic densities (Fig. 13 of Ref. 39), it yields the same lattice constants and bulk moduli.

[61]J. Callaway, X. Zou, and D. Bagayoko, Phys. Rev. B **27**, 631 (1983). This linear combination of Gaussian orbitals calculation for bcc Li yields a LSD lattice constant of 6.52 bohrs and a LSD bulk modulus of 13.8 GPa. However, a refinement of the same calculation by J. C. Boettger and S. B. Trickey [Phys. Rev. B **32**, 3391 (1985)] yields a LSD lattice constant of 6.32 bohrs and a LSD bulk modulus of 15.8 GPa. Boettger and Trickey estimate that the LSD lattice constant for the ε_c parametrization of Ref. 60 would be 6.35 bohrs in good agreement with the LSD values of our Table IX.

[62]S. H. Wei and H. Krakauer, Phys. Rev. Lett. **55**, 1200 (1985); S. H. Wei, H. Krakauer, and M. Weinert, Phys. Rev. B **32**, 7792 (1985) and references therein.

[63]W. B. Pearson, Can. J. Phys. **32**, 708 (1954).

[64]R. A. Felice, J. Trivisonno, and D. E. Schuele, Phys. Rev. B **16**, 5173 (1977).

[65]H. G. Smith, Phys. Rev. Lett. **58**, 1228 (1987).

[66]M. E. Diederich and J. Trivisonno, J. Phys. Chem. Solids **27**, 637 (1966).

[67]J. F. Nye, *Physical Properties of Crystals* (Clarendon, Oxford, 1985), pp. 145 and 147.

[68]D. Singh, D. P. Clougherty, J. M. MacLaren, R. C. Albers, and C. S. Wang, Phys. Rev. B **44**, 7701 (1991).

[69]J. F. Janak, Phys. Rev. **16**, 255 (1977).

[70]D. Singh and J. Ashkenazi (unpublished).

[71]D. Singh, W. E. Pickett, R. E. Cohen, D. A. Papaconstantopoulos, and H. Krakauer, Physica B **163**, 470 (1990).

[72]V. Sahni, J. Gruenebaum, and J. P. Perdew, Phys. Rev. B **26**, 4371 (1982). A plot of s [Eq. (7)] in bulk Cu is given in Ref. 96.

[73]J. P. Perdew, H. Q. Tran, and E. D. Smith, Phys. Rev. B **42**, 1627 (1990).

[74]H. B. Shore and J. H. Rose, Phys. Rev. Lett. **66**, 2519 (1991). The "ideal metal" described in this paper has the same surface properties as the "stabilized jellium" of Ref. 73, but different bulk properties. J. M. Soler [Phys. Rev. Lett. **67**, 3044 (1991)] has pointed out that the "ideal metal" is not truly stable. "Stabilized jellium," on the other hand, has a realistic bulk modulus (Ref. 73). Neither model is wedded to a density-functional approach.

[75]R. Monnier and J. P. Perdew, Phys. Rev. B **17**, 2595 (1978).

[76]C. Fiolhais and J. P. Perdew, Phys. Rev. B **45**, 6207 (1992).

[77]E. Wikborg and J. E. Inglesfield, Solid State Commun. **16**, 335 (1975).

[78]D. C. Langreth and J. P. Perdew, Phys. Rev. B **15**, 2884 (1977); J. P. Perdew, D. C. Langreth, and V. Sahni, Phys. Rev. Lett. **38**, 1030 (1977); D. C. Langreth and J. P. Perdew, Phys. Lett. A **92**, 451 (1982).

[79]D. C. Langreth and J. P. Perdew, Phys. Rev. B **26**, 2810 (1982); V. Sahni and K. P. Bohnen, *ibid.* **29**, 1045 (1984); M. Rasolt and D. J. W. Geldart, *ibid.* **25**, 5133 (1982).

[80]Z. Y. Zhang, D. C. Langreth, and J. P. Perdew, Phys. Rev. B **41**, 5674 (1990).

[81]X. P. Li, R. J. Needs, R. M. Martin, and D. M. Ceperley, Phys. Rev. B **45**, 6124 (1992).

[82]H. B. Michaelson, J. Appl. Phys. **48**, 4729 (1977).

[83]W. R. Tyson and W. A. Miller, Surf. Sci. **62**, 267 (1977).

[84]J. P. Perdew, Y. Wang, and E. Engel, Phys. Rev. Lett. **66**, 508 (1991).

[85]E. Krotscheck and W. Kohn, Phys. Rev. Lett. **57**, 862 (1986); E. Krotscheck, W. Kohn, and G.-X. Qian, Phys. Rev. B **32**, 5693 (1985).

[86]H. L. Skriver and N. M. Rosengaard, Phys. Rev. B **43**, 9538 (1991).

[87]E. Chacón and P. Tarazona, Phys. Rev. B **37**, 4020 (1988).

[88]J. P. Perdew, Phys. Rev. B **37**, 6175 (1988). Some conclusions are revised by E. Engel and J. P. Perdew, *ibid.* **43**, 1331 (1991), and by Ref. 84.

[89]J. P. Perdew and G. Rosensteel, Mod. Phys. Lett. B **5**, 1081 (1991).

[90]M. K. Harbola and V. Sahni, Phys. Rev. Lett. **62**, 489 (1989); V. Sahni, Surf. Sci. **213**, 226 (1989).

[91]J. C. Slater, *The Self-Consistent Field for Molecules and Solids* (McGraw-Hill, New York, 1974).

[92]D. Mearns, Phys. Rev. B **138**, 5906 (1988); K. Schönhammer and O. Gunnarsson, *ibid.* **37**, 3128 (1988); D. Mearns and W. Kohn, *ibid.* **39**, 10 669 (1989).

[93]U. von Barth, Phys. Rev. A **20**, 1693 (1979).

[94]T. Ziegler, Chem. Rev. **91**, 651 (1991).

[95]A. Becke (unpublished); R. Merkle, A. Savin, and H. Preuss (unpublished); N. M. Harrison, V. R. Saunders, E. Aprà, M. Causa, and R. Dovesi, J. Phys. Condens. Matter **4**, L261 (1992).

[96]O. Gunnarsson, M. Jonson, and B. I. Lundqvist, Phys. Rev. B **20**, 3136 (1979).